2013

Analysis of the Molecular Pathogenesis of Cardiomyopathy-Causing cTnT Mutants I79N, #E96, and #K210

Fan Bai, Hannah Caster, Jose Pinto, and Masataka Kawai

Analysis of the Molecular Pathogenesis of Cardiomyopathy-Causing cTnT Mutants I79N, ΔE96, and ΔK210

Fan Bai,[†] Hannah M. Caster,[†] Jose R. Pinto,[‡] and Masataka Kawai[†*]
[†]Departments of Anatomy and Cell Biology, and Internal Medicine, The University of Iowa, Iowa City, Iowa; and [‡]Department of Biomedical Sciences, The Florida State University, College of Medicine, Tallahassee, Florida

ABSTRACT Three troponin T (TnT) mutants that cause hypertrophic, restrictive, and dilated cardiomyopathy (I79N, ΔE96, and ΔK210, respectively), were examined using the thin-filament extraction/reconstitution technique. Effects of Ca^{2+}, ATP, phosphate, and ADP concentrations on force and its transients were studied at 25°C. Maximal Ca^{2+} tension (T_{HC}) and Ca^{2+}-activatable tension (T_{act}), respectively, were similar among I79N, ΔE96, and WT, whereas ΔK210 led to a significantly lower T_{HC} (~20% less) and T_{act} (~25% less) than did WT. In pCa solution containing 8 mM Pi and ionic strength adjusted to 200 mM, the Ca^{2+} sensitivity (pCa_{50}) of I79N (5.63 ± 0.02) and ΔE96 (5.60 ± 0.03) was significantly greater than that of WT (5.45 ± 0.04), but the pCa_{50} of ΔK210 (5.54 ± 0.04) remained similar to that of WT. Five equilibrium constants were deduced using sinusoidal analysis. All three mutants showed significantly lower K_0 (ADP association constant) and larger K_4 (equilibrium constant of force generation step) relative to the corresponding values for WT. I79N and ΔK210 were associated with a K_2 (equilibrium constant of cross-bridge detachment step) significantly lower than that of ΔE96 and WT. These results demonstrated that at pCa 4.66, the force/cross-bridge is ~18% less in I79N and ~41% less in ΔK210 than that in WT. These results indicate that the molecular pathogenesis of the cardiac TnT mutation-related cardiomyopathies is different for each mutation.

INTRODUCTION

Cardiac troponin T (cTnT) is the tropomyosin (Tm)-binding subunit of the troponin (Tn) complex, but cTnT has many more complex functions than simply tethering Tm to Tn (1). The latter also include the Ca^{2+}-binding subunit (cTnC) and the subunit that inhibits the actomyosin (AM) interaction (cTnI) (2–4). In addition to regulating the AM interaction via Tm, cTnT is now known to interact with actin, whereby it may affect actin-Tm binding (5). cTnT has also been reported to play a critical role in sarcomere assembly (6). The phosphorylation of cTnT is known to affect normal function of cardiac muscle fibers (myocardium) (7). So far, 49 cTnT mutations have been identified and related to various forms of cardiomyopathy: familial hypertrophic cardiomyopathy (HCM), dilated cardiomyopathy (DCM), and restrictive cardiomyopathy (RCM) (8). This diversity in disease implies that cTnT is involved in multiple physiological processes. Notably, mutations in cTnT account for 15% of all HCM cases (8), and HCM patients carrying mutations in cTnT have a much higher incidence of sudden cardiac death (SCD) at an early age than do HCM patients who carry mutations in other sarcomeric proteins (8,9).

I79 lies near a putative Tm-binding region of cTnT (10). A patient study indicated that the I79N lesion causes a high rate of SCD in young adults and that the prognosis in these cases is poor (11). However, the reported effects of I79N have been conflicting, in the cases of both in vitro and in vivo studies. For example, I79N was reported to increase Ca^{2+} sensitivity (pCa_{50}) in adult rats expressing an embryonic form of rat cTnT-I79N (12), yet pCa_{50} was not affected in an ATPase assay carried out with rat cTnT-I79N (13). An in vitro motility assay showed that I79N increased the sliding velocity (13). Transgenic mice harboring a human cTnT-I79N mutation showed neither hypertrophy nor shortened survival (14). Skinned fibers from these transgenic mice showed an increase in pCa_{50}, a decrease in maximum tension and ATPase activity, and an increase in the rates of force activation and relaxation (14).

E96 is located within the Tm-binding region of cTnT (10). Patients carrying the ΔE96 mutation feature both diastolic and systolic dysfunction, and the prognosis is severe (15). Fibers reconstituted with the ΔE96 mutant exhibited an increased pCa_{50} and impaired muscle relaxation, but the maximal force generated did not differ significantly from that in fibers reconstituted with the WT protein (16).

K210 is located in a highly charged region in the IT arm, which is a rigid coiled-coil structure in the Tn complex where TnI and TnT bind, and which is a part of the core domain of the Tn complex and is in close contact with a highly charged region of cTnI (17). Two hydrogen bonds (cTnT E214-cTnI R98 and cTnT R216-cTnI D105) have been shown to stabilize the IT interaction (17). Patients with the ΔK210 mutation manifest severe clinical disease, including a significant incidence of early SCD (18). Functional analysis has demonstrated that ΔK210 results in decreases in pCa_{50}, maximal ATPase activity, and force generated by the affected cardiac fibers (19,20). However, analysis of a transgenic mouse model of ΔK210 showed that pCa_{50} was decreased but that the maximal force was not decreased (21). A recent study also showed that ΔK210 led to changes in the phosphorylation status of

Submitted November 26, 2012, and accepted for publication April 2, 2013.
*Correspondence: masataka-kawai@uiowa.edu
Editor: K. W. Ranatunga.

0006-3495/13/05/1979/10 $2.00
http://dx.doi.org/10.1016/j.bpj.2013.04.001

several sarcomeric proteins, including cMyBP-C, cTnT, and cTnI, indicating that the consequences of the ΔK210 mutation go far beyond the IT interaction (22).

The literature regarding Tn mutations and their roles in disease and muscle regulation is extensive. Previous studies have focused on measurement of three parameters: Ca^{2+} sensitivity (pCa_{50}), maximal force (T_{HC}), and force during relaxation (T_{LC}). Based on these analyses, it is believed that the Tn mutations that cause hypertrophic and restrictive cardiomyopathy lead to an increase in pCa_{50}, whereas the mutations that cause dilated cardiomyopathy lead to decreased pCa_{50} (8). However, none of those studies evaluated the cross-bridge kinetics, which affect the ability of myosin to generate force and are hence essential in characterizing early pathogenesis that leads to cardiomyopathy.

In this study, the thin-filament extraction/reconstitution technique was used instead of the traditional Tn replacement technique. The latter has been used extensively by investigators and shown to be a reliable technique for studying Tn functions (7,23–25). Our thin-filament extraction/reconstitution technique, although more invasive than the Tn replacement technique, has been shown to fully restore isometric tension, Ca^{2+} sensitivity, cooperativity, apparent rate constants, and kinetic constants of the elementary steps of the cross-bridge cycle (26–28) (see Supporting Material for a detailed comparison of these two methods). We have further evaluated the reconstituted fibers using SDS-PAGE (29) and electron microscopy (26), with satisfactory results. After thin-filament reconstitution, the effects of three cardiomyopathy-linked cTnT mutants on isometric tension, stiffness, and cross-bridge kinetics were studied using sinusoidal analysis.

Our results are as follows: 1), all three cTnT mutants caused significantly accelerated ADP dissociation from the myosin head; 2), I79N and ΔK210 caused a decrease in the cross-bridge detachment rate and an increase in the number of actively cycling cross-bridges; 3), I79N and ΔE96 caused a significant increase in pCa_{50} without altering the maximum force, but ΔK210 caused a decrease in maximum force with unchanged pCa_{50}. These results are discussed in the context of the early pathogenesis of each mutation.

MATERIALS AND METHODS

Experimental materials and the thin-filament extraction/reconstitution technique

Small bundles (length ~10 mm, diameter ~1–2 mm) of bovine trabecular muscles were dissected from right ventricles and chemically skinned (28). On the day of experiments they were further split into thin bundles (length ~2 mm, diameter 90–110 μm), mounted in the experimental apparatus, and stretched to a sarcomere length of ~2.1 μm. Thin-filament extraction and reconstitution were performed as described previously (30), as originally developed in the Ishiwata laboratory (27) and refined in the Kawai laboratory (26) (Fig. S1 in the Supporting Material). The protein concentrations used were 1.5 mg/ml actin, 0.33 mg/ml Tm, and 0.78 mg/ml Tn (28).

Proteins

Rabbit skeletal-muscle G-actin was purified as described elsewhere (31). Bovine cardiac Tm and Tn were purified from fresh cow hearts, as described elsewhere (32). Both proteins were purified in the Kawai laboratory. Human WT and mutant cTnT, human cTnI, and human cTnC were expressed as recombinant proteins in *E. coli* and purified in the Potter laboratory. The WT and mutant cTn complex proteins used for reconstitution were 97–99% pure (16).

Experimental solutions

Solutions were prepared as described (30). In the case of pCa solution, two sets of solutions were used, one at 8 mM Pi and 200 mM ionic strength (IS) (30) and the other at 0 mM Pi and 150 mM IS (33). I79N and ΔE96 were studied only in the 8 mM Pi pCa solutions, whereas ΔK210 was studied in both pCa solutions.

Tension normalization

All tension values were normalized to T_a, the tension of actin-filament reconstituted fibers in the absence of Tm and Tn, and in standard activating solution (8 mM Pi and IS 200 mM) (30). This solution closely mimics the physiological environment in cardiomyocytes, in which [Pi] during contraction was reported to be ~6 mM (34) and IS ~215 mM (35). The reason for using T_a instead of the absolute tension in Pascals is that this minimizes the scatter of data stemming from error in estimating the cross-sectional area of the fibers. In this study, T_a averaged to 13.8 ± 0.7 kPa ($N = 63$). T_a increased 1.5-fold on reconstitution with Tm and Tn (26–28), twofold when Pi was deleted from the activating saline (30,36), and 1.2-fold when IS was reduced from 200 mM to 150 mM (37,38), as has often been done in experiments performed by other investigators. Multiplication of these values by the T_a results in a value of 50 kPa (13.8 kPa × 1.5 × 2 × 1.2), consistent with the range of values reported for rat cardiac muscle fibers (39–75 kPa) (39,40).

pCa-tension study

The pCa-tension study was performed as described previously (41) across a pCa range of 8.0–4.66. The tension and stiffness at pCa 8.0 (low Ca^{2+}) are termed T_{LC} and Y_{LC}, respectively; the stiffness is defined as Y_∞ (42), but the ∞ symbol is dropped for simplicity. The tension and stiffness at pCa 4.66 (high Ca^{2+}) are referred to as T_{HC} and Y_{HC}, respectively. The baseline tension was measured in super-relaxing solution (30) at 0°C, in the presence of 6 mM EGTA, 5 mM MgATP, and 40 mM BDM; neither tension nor cross-bridge cycling are significant under this condition. The pCa-tension relationship was fitted to the Hill equation:

$$\text{Tension} = \frac{T_{act}}{1 + \left(\frac{Ca_{50}}{[Ca^{2+}]}\right)^{n_H}} + T_{LC}, \quad (1)$$

where $pCa = -\log_{10}[Ca^{2+}]$, T_{act} is the Ca^{2+}-activatable tension, and Ca_{50} is the apparent Ca^{2+} dissociation constant, which represents the Ca^{2+} concentration at half tension. pCa_{50} ($-\log_{10}Ca_{50}$) represents Ca^{2+} sensitivity, and n_H (the Hill factor) represents cooperativity. $T_{HC} = T_{act} + T_{LC}$ is the tension at high $[Ca^{2+}]$. pCa-tension curves were individually fitted to Eq. 1, and the fitted parameters were averaged. All experiments were carried out at 25°C.

Sinusoidal analysis

The elementary steps of the six-stage cross-bridge cycle (Fig. S2) were studied using sinusoidal analysis as described previously (42,43).

RESULTS

pCa-tension studies

To demonstrate the integrity of our preparations and the effectiveness of our method, we first studied the pCa-tension relationship in native bovine cardiac muscle fibers (Fig. 1, *dashed curves with open circles*) and thin filaments reconstituted with actin, Tm, and the Tn complex purified from bovine ventricle (Fig. 1, *curves with solid squares*). Notably, the two plots are almost identical, and when the data were fitted to Eq. 1, we obtained $pCa_{50} = 5.69 \pm 0.01$ and $n_H = 3.22 \pm 0.18$ (mean ± SE, $N = 14$) for native fibers, and $pCa_{50} = 5.68 \pm 0.02$ and $n_H = 2.71 \pm 0.23$ ($N = 9$) for thin-filament-reconstituted fibers. The values for these parameters are not significantly different. The reproducibility of tension in thin-filament-reconstituted fibers was 104 ± 3% ($N = 38$), which is not statistically different from 100%.

To determine the effects of cardiomyopathy-related cTnT mutants on T_{LC}, T_{HC}, pCa_{50}, and n_H, we studied the pCa-tension relationship of the thin-filament-reconstituted myocardium. Fig. 2 shows pCa-tension plots for mutant and WT cTnTs. The results of the experiments, which were carried out at 8 mM Pi, are plotted in Fig. 3. T_{act} of I79N (Fig. 2 *A*) appears larger than that of WT, but the difference is insignificant. T_{act} of ΔE96 (Fig. 2 *B*) is nearly identical to that of WT, but pCa_{50} of ΔE96 appears slightly larger than that of WT. T_{act} of ΔK210 (Fig. 2 *C*) appears to be significantly smaller than that of WT.

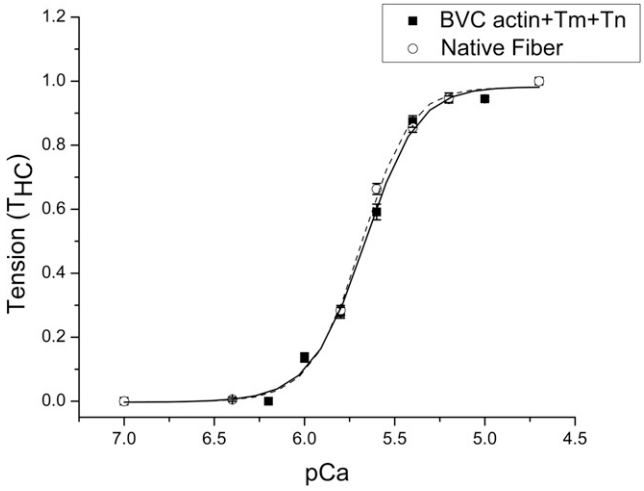

FIGURE 1 pCa-tension plot comparing native cardiac muscle fibers (*dashed curves with open circles*) and fibers reconstituted with bovine cardiac actin, Tm, and Tn (*curves with solid squares*). Normalized tension is plotted against pCa. The symbols represent the data points and the curves represent the best fit to Eq. 1. Error bars represent the mean ± SE, but most are smaller than the symbol size. The pCa_{50} value was identical between native fibers (5.69 ± 0.01, N=14) and fibers reconstituted with bovine cardiac actin, Tm, and Tn (5.68 ± 0.02, N=9). Although the cooperativity of actin, Tm, and Tn-reconstituted myocardium (2.71 ± 0.23, N=9) was slightly less than that of native fibers (3.22 ± 0.18, N=14), this difference was not statistically significant.

The results for pCa-tension were fitted to Eq. 1; the average values of parameters are listed in Table S1 and plotted in Fig. 3. None of the three cTnT mutants showed significant changes in T_{LC} compared to WT (Fig. 3 *A*). With respect to maximal force, T_{HC} values for I79N (1.82 ± 0.13 T_a) and ΔE96 (1.66 ± 0.14 T_a) were similar to that of WT (1.68 ± 0.13 T_a), but T_{HC} for ΔK210 (1.33 ± 0.12 T_a) was significantly lower than that of WT. T_{act} followed the general pattern observed for T_{HC}. The Y_{LC}s of ΔE96 and ΔK210 were similar to that of WT, but Y_{LC} of I79N was significantly less than that of WT (Fig. 3 *B*). Y_{HC} was similar in all genotypes studied, but Y_{act} of I79N was significantly larger than that of the others. Cooperativity was calculated by averaging individual n_H values (Fig. 3 *C*). Only I79N (2.53 ± 0.22) showed significantly increased n_H compared to that of WT (1.71 ± 0.18). The pCa_{50} values for I79N (5.63 ± 0.02, $N = 16$) and ΔE96 (5.60 ± 0.03) were significantly larger than that of WT (5.45 ± 0.04), indicating increased Ca^{2+} sensitivity, whereas that of ΔK210 (5.54 ± 0.04) did not differ significantly from that of WT (Fig. 3 *D*).

Although our results demonstrate that pCa_{50} is not significantly different between ΔK210 and WT, previous reports have shown a decrease in pCa_{50} with this mutant (19,20,44). One reason for this apparent disagreement is that the solutions used were different. Whereas we used solutions at 8 mM Pi and IS 200 mM, previous investigators used solutions without added Pi and IS at 150 mM. For this reason, we also studied ΔK210 and WT in solution at 0 mM Pi and IS 150 mM (see Fig. 2 *D*). When Fig. 2, *C* and *D*, are compared, the decreases in [Pi] (from 8 mM to 0 mM) and IS (from 200 mM to 150 mM) shifted the pCa-tension curves to the left (increase in pCa_{50}), decreased the slope (reduced cooperativity), and increased T_{HC} significantly and as reported previously (45). When compared at 0 Pi and IS 150 mM, ΔK210 caused a significant decrease in T_{HC} (2.74 ± 0.27 T_a, $N = 6$) compared to that in WT (3.62 ± 0.33 T_a, $N = 6$). The pCa_{50} of ΔK210 (5.65 ± 0.06, $N = 6$) was significantly less than that of WT (5.89 ± 0.03, $N = 6$), consistent with findings from previous studies (19,21,44). The cooperativity of ΔK210 (1.29 ± 0.21, $N = 6$) was significantly less than that of WT (1.90 ± 0.15, $N = 6$).

Sinusoidal analysis and cross-bridge kinetics

Sinusoidal analysis was performed to characterize the elementary steps of the cross-bridge cycle (Fig. S2) in the reconstituted myocardium (26,42). The apparent rate constants $2\pi b$ and $2\pi c$ were measured as functions of [Pi] and [MgATP] (Fig. 4). All mutants exhibited some differences in $2\pi c$ relative to the WT value (Fig. 4, *A–C*), but these differences were small. I79N and ΔE96 caused a large increase in $2\pi b$ compared to that observed in the WT and ΔK210 preparations (Fig. 4, *D–F*). The rate and association

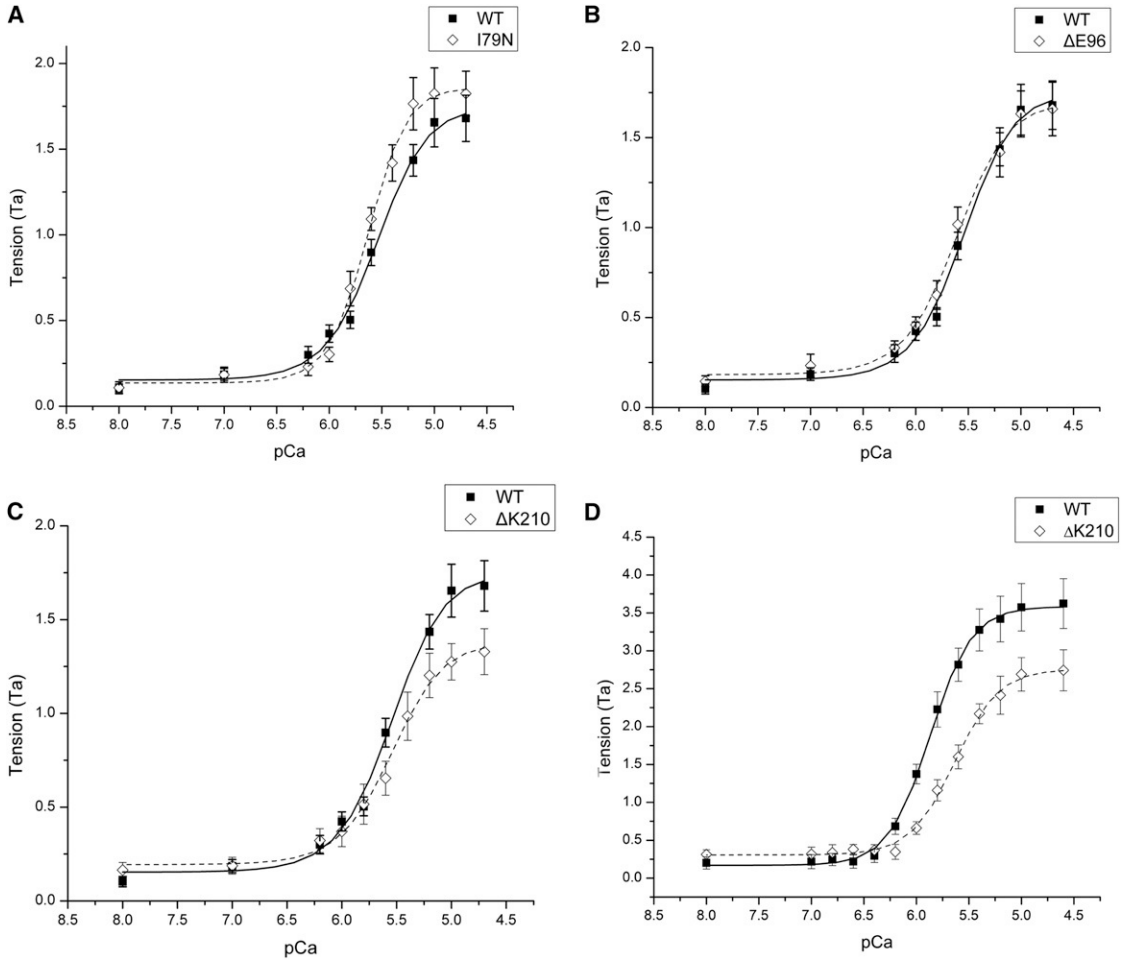

FIGURE 2 pCa-tension plots comparing WT and three mutant forms of TnT. The mean ± SE values for 12–20 experiments are shown. (*A–C*) pCa-tension curves for the mutants and WT at IS 200 mM and 8 mM Pi. (*D*) Curves for ΔK210 and WT at IS 150 mM and 0 mM Pi. Tension is normalized to $T_a = 13.79 \pm 0.73$ kPa ($n = 63$).

constants of the elementary steps as defined in the cross-bridge model (Fig. S2) are collectively referred to as kinetic constants and were deduced by fitting the dependence of apparent rate constants on ligand concentrations to Eqs. S2–S4. The kinetic constants for the mutant and WT proteins are compared in Fig. 5. All kinetic constants changed to some extent in the mutants, but the only changes that were significant ($p < 0.05$) were as follows. All three TnT

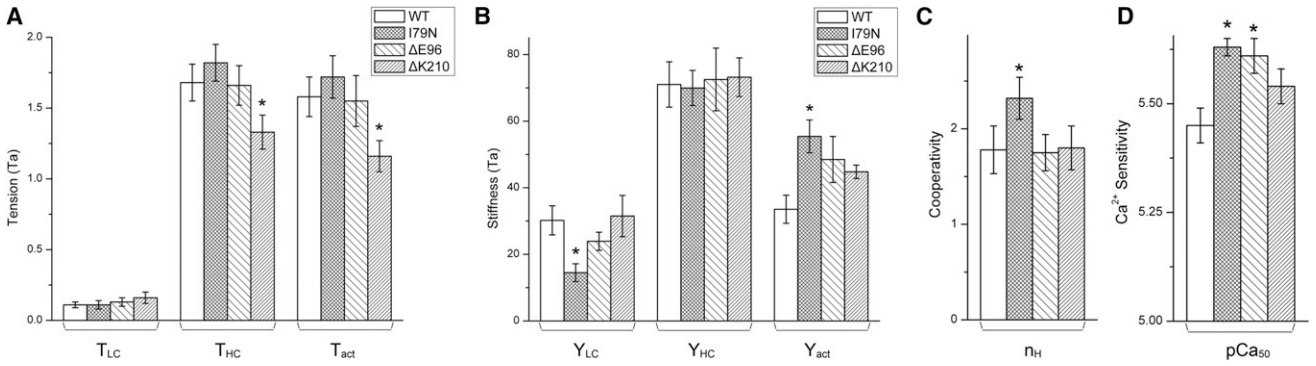

FIGURE 3 Results of pCa-tension studies. (*A*) Isometric tension: T_{HC}, T_{act}, and T_{LC} are as defined in Eq. 1. (*B*) Stiffness. (*C*) Cooperativity. (*D*) pCa_{50}. Tension and stiffness were normalized to T_a. $^*p < 0.05$.

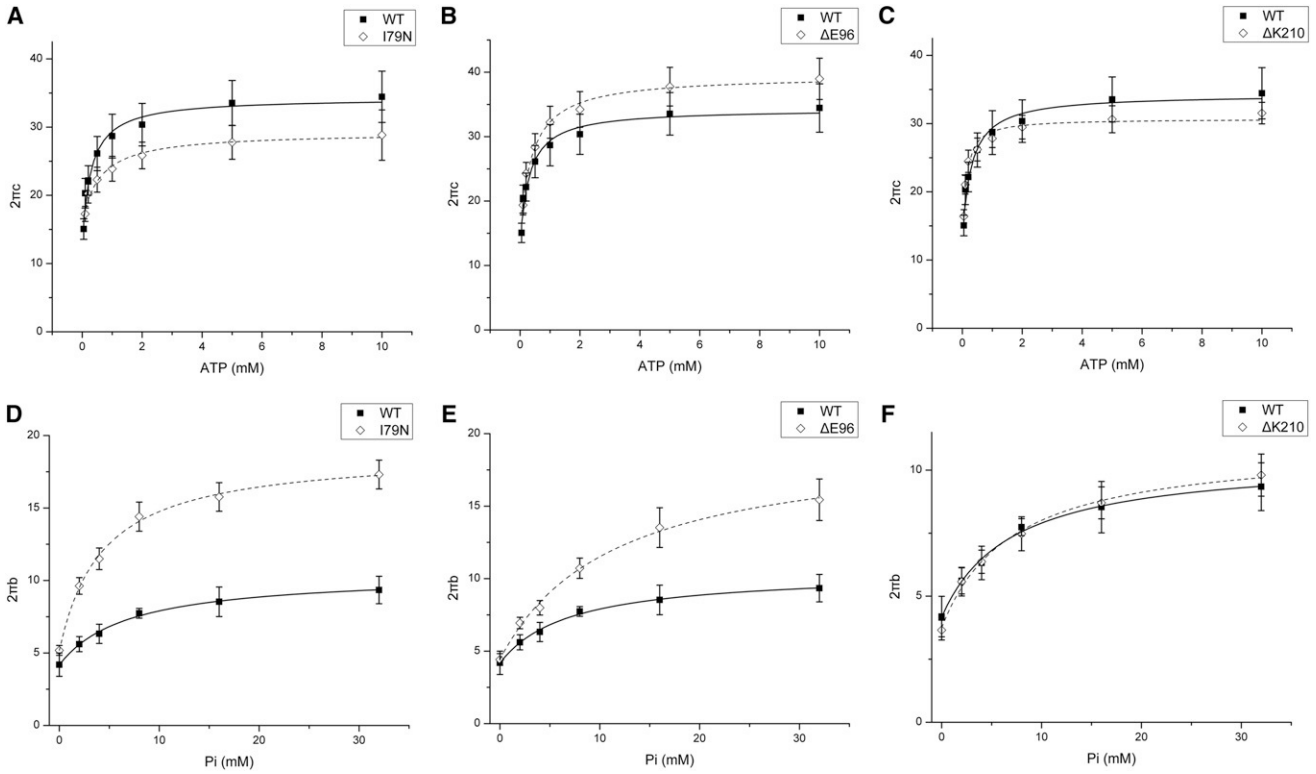

FIGURE 4 Apparent rate constants. (*A–C*) $2\pi c$ is plotted against [MgATP]. (*D–F*) $2\pi b$ is plotted against [Pi]. Mean ± SE values are shown for 9–19 experiments. Solid curves are the best fit of the data to Eqs. S2–S4 (69).

mutants showed a significant decrease in K_0, the ADP association constant (I79N, 30 ± 2 mM^{-1}; ΔE96, 35 ± 4 mM^{-1}; ΔK210, 27 ± 3 mM^{-1}), and a significant increase in K_4, the force-generation step (I79N, 0.70 ± 0.06; ΔE96, 0.28 ± 0.01; ΔK210, 0.85 ± 0.12) compared to WT ($K_0 = 47 \pm 1$ mM^{-1} and $K_4 = 0.21 \pm 0.03$). The I79N and ΔK210 exhibited a significant decrease in K_2, the cross-bridge detachment step (I79N, 0.80 ± 0.11; ΔE96, 0.85 ± 0.13) compared to that of ΔE96 (1.74 ± 0.24) and WT (1.48 ± 0.26). K_1, the ATP association constant, remained similar among the mutant and WT preparations, as did K_5 (Pi association constant). k_2, the forward rate constant of the cross-bridge detachment step, decreased significantly in I79N (14.4 ± 1.8 s^{-1}) and ΔK210 (15.9 ± 1.5s^{-1}) compared to WT (21.4 ± 0. 3s^{-1}), but increased significantly in ΔE96 (27.0 ± 3.8 s^{-1}). k_4,

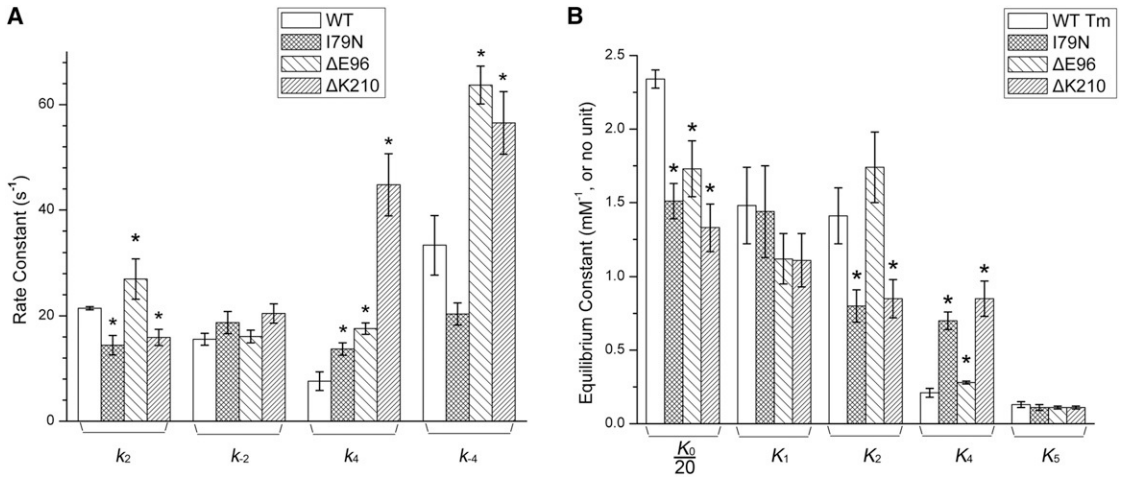

FIGURE 5 Comparison of the kinetic constants. (*A*) Rate constants. (*B*) Equilibrium constants.

the rate constant of the force-generation step, increased significantly in all mutants (I79N,13.7 ± 1.2 S^{-1}; ΔE96, 17.6 ± 1.1S^{-1}; ΔK210, 44.8 ± 5.9S^{-1}) compared to WT (7.6 ± 1.8S^{-1}).

Cross-bridge distribution and force/cross-bridge

There are two possible explanations for the change observed in isometric tension (Fig. 3 *A*): a change in the number of force-generating cross-bridges, or a change in the force generated per cross-bridge. For this reason, the distribution of cross-bridges in each state under standard activating conditions (30) was calculated using the observed kinetic constants as described previously (46); the results are shown in Fig. 6. Also included is the probability of a strongly attached (force-generating) state (Att), where Att = AMD + AM + AM*S + AM*DP + AM*D = 1 − Det. There were no significant effects of mutations in the three left-side states (AMD, AM, AM*S), and significant changes were limited to three right-side states (Det, AM*DP, AM*D). I79N and ΔK210 caused significant decreases in the detached state (Det, I79N, 24.9 ± 1.3%; ΔK210, 23.1 ± 1.4%) compared to the WT (43.4 ± 2.3%), and these were countered by significant increases of the AM*DP state (I79N, 17.4 ± 0.9%; ΔK210, 19.7 ± 1.6%) and the AM*D state (I79N, 19.8 ± 2.9%; ΔK210, 22.4 ± 1.8%) compared to the corresponding states for WT (AM*DP, 9.1 ± 1.1%; AM*D, 8.7 ± 1.2%). These changes resulted in significant increases in the Att state. I79N and ΔK210 showed an ~33% increase in the number of force-generating cross-bridges (I79N, 75.1 ± 1.3%; ΔK210, 76.8 ± 1.4%) relative to the number for WT (56.6 ± 2.3%). ΔE96 showed a cross-bridge distribution similar to that in WT. These results demonstrate that at pCa 4.66, the T_{HC}/cross-bridge (T_{HC}/(Att)) in I79N is 2.4 ± 0.2 T_a and ~18% less than that of WT (3.0 ± 0.3 T_a), and T_{HC}/(Att) in ΔK210 it is 1.7 ± 0.1 T_a and ~41% less than that of WT, but that T_{HC}/X_{att} in ΔE96 is 2.9 ± 0.3 T_a and similar to that of WT.

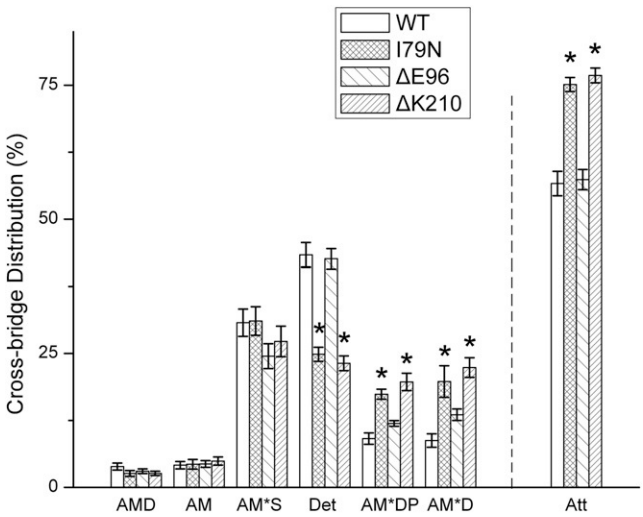

FIGURE 6 Cross-bridge distribution. The kinetic constants were used to calculate the cross-bridge distribution over six states under the standard activating condition (5 mM MgATP, 8 mM Pi, 0.02 mM MgADP, and pCa 4.66). Att indicates the sum of all strongly attached (force-generating) cross-bridges. The distribution was calculated individually and averaged for 9–13 fibers.

DISCUSSION

As a key component of the cardiac excitation-contraction coupling, TnT is responsible for holding Tm in its inhibitory position in the absence of Ca^{2+} and thereby for blocking the AM interaction (47). TnT interacts with Tm in the presence of Ca^{2+}, and moves Tm into the closed position, which permits some cross-bridges to attach (1). The attached cross-bridges further shift Tm to the open position, permitting more cross-bridges to be strongly attached to actin (26,32,48–51). E96 of cTnT is located within the Tm-binding region, and I79 is located next to this region (10). A mutation in TnT may shift the Tm position and affect the otherwise strong interaction between actin and myosin. Our earlier results demonstrated that the presence/absence of Tm (26), as well as point mutations of Tm (30,45), modify the force/cross-bridge and cross-bridge kinetics.

Earlier studies have demonstrated that in the context of cardiomyopathy-causing Tm mutants, T_{LC} is abnormal. In HCM this value is increased (30), and in DCM (45) it is decreased. Because of these findings, we focused on T_{LC}, assessing whether the same trend is observed with the TnT mutants. However, none of the three cTnT mutants exhibited abnormal T_{LC} (Fig. 3 *A*) despite the differences in phenotype with which they are associated. These observations imply that the blocked state of Tm is not affected in the three cTnT mutants.

As shown by patient studies (11,15,18), the three cTnT mutants lead to three different phenotypes and are associated with a prognosis more severe than that for disease caused by mutations in other sarcomeric proteins. All three cTnT mutants caused a significant increase in dissociation of ADP from the myosin head (decreased K_0, Fig. 5 *B*), which suggests that the shortening velocity is faster. A previous study reported a doubling of the shortening velocity in I79N (52), but the shortening velocity has not been measured in ΔE96 and ΔK210. The increases in pCa_{50} in I79N and ΔE96 (Table S1) are smaller than those reported for Tm mutants (30), whose consequences are not as serious as those reported for TnT mutants. Therefore, the poor prognosis for patients harboring these mutations may result from the combination of a change in pCa_{50} and alterations in cross-bridges kinetics. The elementary steps of the cross-bridge cycle are severely disturbed by these mutations (Table S1 and Fig. 5). Our investigation demonstrates that cTnT has far more influence on disease pathogenesis than

merely regulating the AM interaction. Indeed, cTnT has been shown to alter the posttranslational modification of other sarcomeric proteins (22). Therefore, cTnT carries more functions than a regulatory protein, which may help to explain the poor prognosis of human patients carrying cTnT mutations.

One of the controversies regarding the study of cTnT mutations is that the values obtained for maximal force have been highly variable. Moreover, the results obtained from Tn-reconstitution assays for HCM mutations have often been inconsistent with those from transgenic animals (14,16,53–56). Our earlier study showed that tension recovery can be affected by the solution systems used by different researchers (45). In the case of transgenic animals, posttranslational modifications and isoform switching of the contractile proteins may influence outcomes (22,57,58). Since the maximal force varies among preparations (16,52,59,60), pCa_{50} should be considered a fingerprint that identifies those Tn mutations that affect regulation. The results we report here are consistent with the established Ca^{2+}-sensitivity paradigm.

One important feature of this study of cTnT is that it investigates how mutations within a single protein disrupt cardiac function in ways that lead to three phenotypes. Are these phenotypes caused by different compensatory mechanisms, or initiated by different molecular mechanisms as a result of a change in cTnT (61,62)? The fact that each mutation produced different results indicates that each mutation should be considered independently of the others.

I79N

I79N results in the HCM phenotype, and it is associated with a significant decrease in the equilibrium constant of the cross-bridge detachment step (Fig. 5 *B*), a 20% decrease in force/cross-bridge (T_{HC}/X_{att}), significant increases in pCa_{50} (0.18 ± 0.04 unit) (Fig. 3 *D*), cooperativity (Fig. 3 *C*), and the force-generation rate (k_4 and K_4; Fig. 5). An earlier study in transgenic mice showed that I79N caused a decrease in maximal force and an increase in pCa_{50} (14). Cardiac performance analysis showed an increase in end-diastolic pressure and relaxation time, but no evidence of diastolic dysfunction (63). In our study, the maximal force remained similar to that in WT preparations (comparable T_{HC} and T_{act} among I79N and WT; Fig. 3 *A*), demonstrating that this mutation does not immediately result in a decrease in contractility. This result is consistent with the findings using skinned fibers (55). The decrease in maximal force may be caused by secondary effects of the mutation, such as changed phosphorylation levels, as mentioned below for ΔK210. Our kinetic analysis further revealed that I79N caused an increase in the number of Att states (Fig. 6), compensating for the decreased force/cross-bridge and maintaining normal force. Thus, at the molecular level, there may be a compensatory mechanism that maintains normal overall force. The decrease in force/cross-bridge indicates that the normally strong binding between actin and myosin is weakened in I79N. The cross-bridge detachment rate (k_2) is decreased in I79N, which may appear inconsistent with an earlier observation that the rate of relaxation (g) increased in the I79N transgenic mouse model (14). However, this difference is a consequence of using different models; given that we used a realistic six-state model and the earlier report was based on a two-state model, g must be a composite of multiple steps.

ΔE96

ΔE96 results in the RCM phenotype, but it did not significantly influence many of the parameters we have studied, except for the ADP dissociation constant (a decrease in K_0), cross-bridge detachment rate (an increase in k_2), and the kinetic constants of the force-generation step (increase in k_4, k_{-4}, and K_4) (Fig. 5). ΔE96 also increased pCa_{50} by 0.15 ± 0.05 units (Fig. 3 *D*) without changing the maximal force or stiffness (Fig. 3, T_{HC}, T_{act}, Y_{HC}, and Y_{act}). These results are consistent with the hypothesis that the charged residue E96 is involved in the activation process. The typical abnormal diastolic filling pattern in RCM patients may be related to the abnormal ventricular-wall stiffness in the context of low Ca^{2+}, with neither tension (T_{LC}) nor stiffness (Y_{LC}) changing (Fig. 3, *A* and *B*). Force/cross-bridge did not change in the context of high Ca^{2+}. A previous study on skinned fibers showed that ΔE96 caused a significant increase in residual unregulated tension (16), but this was not observed in the study presented here. The different solution conditions discussed below may explain this difference.

ΔK210

ΔK210 results in a DCM phenotype, causing significant decreases in the cross-bridge detachment rate (Fig. 5. k_2 and K_2), significant increases in the force-generation rate (Fig. 5, k_4, k_{-4}, and K_4), and significant increases in the probability of Att (Fig. 6). However, neither T_{LC}, pCa_{50}, nor cooperativity changed significantly (Fig. 3). Although K210 lies far from the Tm binding region, its deletion may affect the position of Tm in the open state (49), resulting in partial shielding of the AM interaction and leading to a decrease in the maximal forces (Fig. 3 *A*, T_{HC} and T_{act}) and force/cross-bridge. The decrease in the Ca^{2+} activatable tension (T_{act}) may cause a systolic problem, which explains the emergence of DCM, consistent with findings from previous pathogenesis studies (19,20).

Our observation that pCa_{50} was unchanged by ΔK210 (Figs. 2 *C* and 3 *D*) is at variance with the findings of

previous studies that reported a decrease in pCa_{50} (20,21,44). There are two possible explanations for this disagreement.

1. There is a difference in the pCa solutions used. Our solutions contained 8 mM Pi and IS was adjusted to 200 mM, whereas other investigators (20,21,44) used no added Pi and IS 150 mM. When we used the latter solution, we observed a decrease in pCa_{50} similar to that previously reported (Fig. 2 *D*). In rabbit psoas fibers, elevating IS from 128 mM to 201 mM decreases pCa_{50} by ~0.35 units (64), and increasing [Pi] from 0 to 7.5 mM decreases pCa_{50} by 0.23 units (65). Similar effects of [Pi] on pCa_{50} have also been reported in cardiac fibers (36,66). Consequently, changes in IS and [Pi] will lead to significant changes in the pCa_{50} value and other parameters for both WT and mutant proteins. However, this effect may be different in each mutation. For example, removing Pi and lowering IS caused the pCa_{50} of WT to increase by 0.44 unit. In contrast, the pCa_{50} of ΔK210 only increased by 0.11 unit under the same condition. This difference directly leads to our observation that ΔK210 decreased the Ca^{2+} sensitivity at 0 mM Pi and IS 150 mM. A similar difference was also reported in our recent article on DCM-causing Tm mutants E40K and E54K (45): their pCa_{50} decreased compared to that of WT in the 0 mM Pi and 150 mM IS solutions, whereas pCa_{50} did not change in the 8 mM Pi, IS 200 mM solutions. These Tm mutants introduced a large change in charge that destabilizes Tm's coiled-coil structure. Previous studies on skinned cardiac fibers that used similar 0 mM Pi and low-IS solutions reported an increased Ca^{2+} sensitivity for I79N and ΔE96 mutants of TnT (12,14,16), which qualitatively agrees with our findings. We conclude, therefore, that removing Pi and lowering IS caused similar changes in pCa_{50} among I79N, ΔE96, and the WT. Thus, these two mutants showed similarly increased pCa_{50} values in two sets of pCa solutions.

   It has been reported that physiological conditions in contracting cardiomyoctes include ~4.5 mM ATP, ~6 mM Pi (34,67), and IS ~215 mM (35). Based on the above-described findings, we conclude that pCa_{50} does not differ between ΔK210 and WT under physiological conditions, but that significant differences arise at IS 150 mM and 0 mM Pi. Our solution system is a better approximation of the physiological condition, which may be essential to understanding the physiological consequence of a mutation.
2. The decrease in pCa_{50} may not be the direct result of a mutation, but rather a secondary consequence thereof. A transgenic mouse study showed that in vivo, the ΔK210 mutant was associated with changes in the phosphorylation levels of sarcomeric proteins, including cMyPB-C, cTnT, and cTnI (22). A change in phosphorylation level can have significant consequences for the contractile/regulatory response of the affected myocardium (57,58,68), including a change in the pCa_{50} value. In our studies, the background material (bovine myocardium) is the same, and with the exception of the TnT mutants, the proteins used to reconstitute the thin filament are the same. Consequently, we observe direct effects of the mutation in the absence of masking by other posttranslational modifications. Thus, we suggest that the change in pCa_{50} observed by others in the case of ΔK210 may have been caused by changes in posttranslational modification(s) of sarcomeric proteins. Therefore, we can state that getting at the primary cause is essential to restoring normal function.

CONCLUSION

We conclude that three cTnT mutants (I79N, ΔE96, and ΔK210) lead to distinct molecular pathogenesis, specifically with regard to the mechanisms underlying cross-bridge kinetics and force generation. The different downstream effects eventually lead to the differences in disease phenotype. Although we conclude that a reduced isometric tension is part of the defect and contributes to the disease phenotype, alterations in kinetic constants of the cross-bridge cycle contribute as well and are responsible for the distinctions between the disease phenotypes.

SUPPORTING MATERIAL

One table, three figures, and materials and methods are available at http://www.biophysj.org/biophysj/supplemental/S0006-3495(13)00392-5.

We are grateful to Dr. James D. Potter of the University of Miami, Department of Pharmacology, for providing the regulatory proteins.

This work was supported by grants from the National Institutes of Health (HL70041 to MK, and HL103840 to JRP). The content of this study is solely the responsibility of the authors, and does not necessarily represent the official view of the awarding organization.

REFERENCES

1. Perry, S. V. 1998. Troponin T: genetics, properties and function. *J. Muscle Res. Cell Motil.* 19:575–602.
2. Potter, J. D., and J. Gergely. 1974. Troponin, tropomyosin, and actin interactions in the Ca^{2+} regulation of muscle contraction. *Biochemistry.* 13:2697–2703.
3. Solaro, R. J., and H. M. Rarick. 1998. Troponin and tropomyosin: proteins that switch on and tune in the activity of cardiac myofilaments. *Circ. Res.* 83:471–480.
4. Zot, A. S., and J. D. Potter. 1987. Structural aspects of troponin-tropomyosin regulation of skeletal muscle contraction. *Annu. Rev. Biophys. Biophys. Chem.* 16:535–559.
5. Heeley, D. H., K. Golosinska, and L. B. Smillie. 1987. The effects of troponin T fragments T1 and T2 on the binding of nonpolymerizable tropomyosin to F-actin in the presence and absence of troponin I and troponin C. *J. Biol. Chem.* 262:9971–9978.

6. Sehnert, A. J., A. Huq, …, D. Y. Stainier. 2002. Cardiac troponin T is essential in sarcomere assembly and cardiac contractility. *Nat. Genet.* 31:106–110.
7. Sumandea, M. P., W. G. Pyle, …, R. J. Solaro. 2003. Identification of a functionally critical protein kinase C phosphorylation residue of cardiac troponin T. *J. Biol. Chem.* 278:35135–35144.
8. Willott, R. H., A. V. Gomes, …, J. D. Potter. 2010. Mutations in Troponin that cause HCM, DCM and RCM: what can we learn about thin filament function? *J. Mol. Cell. Cardiol.* 48:882–892.
9. Varnava, A. M., P. M. Elliott, …, W. J. McKenna. 2001. Hypertrophic cardiomyopathy: histopathological features of sudden death in cardiac troponin T disease. *Circulation.* 104:1380–1384.
10. Palm, T., S. Graboski, …, N. J. Greenfield. 2001. Disease-causing mutations in cardiac troponin T: identification of a critical tropomyosin-binding region. *Biophys. J.* 81:2827–2837.
11. Watkins, H., W. J. McKenna, …, C. E. Seidman. 1995. Mutations in the genes for cardiac troponin T and α-tropomyosin in hypertrophic cardiomyopathy. *N. Engl. J. Med.* 332:1058–1064.
12. Rust, E. M., F. P. Albayya, and J. M. Metzger. 1999. Identification of a contractile deficit in adult cardiac myocytes expressing hypertrophic cardiomyopathy-associated mutant troponin T proteins. *J. Clin. Invest.* 103:1459–1467.
13. Lin, D., A. Bobkova, …, L. S. Tobacman. 1996. Altered cardiac troponin T in vitro function in the presence of a mutation implicated in familial hypertrophic cardiomyopathy. *J. Clin. Invest.* 97:2842–2848.
14. Miller, T., D. Szczesna, …, J. D. Potter. 2001. Abnormal contractile function in transgenic mice expressing a familial hypertrophic cardiomyopathy-linked troponin T (I79N) mutation. *J. Biol. Chem.* 276:3743–3755.
15. Peddy, S. B., L. A. Vricella, …, B. L. Loeys. 2006. Infantile restrictive cardiomyopathy resulting from a mutation in the cardiac troponin T gene. *Pediatrics.* 117:1830–1833.
16. Pinto, J. R., M. S. Parvatiyar, …, J. D. Potter. 2008. A troponin T mutation that causes infantile restrictive cardiomyopathy increases Ca^{2+} sensitivity of force development and impairs the inhibitory properties of troponin. *J. Biol. Chem.* 283:2156–2166.
17. Takeda, S., A. Yamashita, …, Y. Maéda. 2003. Structure of the core domain of human cardiac troponin in the Ca^{2+}-saturated form. *Nature.* 424:35–41.
18. Mogensen, J., R. T. Murphy, …, W. J. McKenna. 2004. Severe disease expression of cardiac troponin C and T mutations in patients with idiopathic dilated cardiomyopathy. *J. Am. Coll. Cardiol.* 44:2033–2040.
19. Venkatraman, G., A. V. Gomes, …, J. D. Potter. 2005. Characterization of troponin T dilated cardiomyopathy mutations in the fetal troponin isoform. *J. Biol. Chem.* 280:17584–17592.
20. Venkatraman, G., K. Harada, …, J. D. Potter. 2003. Different functional properties of troponin T mutants that cause dilated cardiomyopathy. *J. Biol. Chem.* 278:41670–41676.
21. Du, C. K., S. Morimoto, …, T. Sasaguri. 2007. Knock-in mouse model of dilated cardiomyopathy caused by troponin mutation. *Circ. Res.* 101:185–194.
22. Sfichi-Duke, L., M. L. Garcia-Cazarin, …, M. P. Sumandea. 2010. Cardiomyopathy-causing deletion K210 in cardiac troponin T alters phosphorylation propensity of sarcomeric proteins. *J. Mol. Cell. Cardiol.* 48:934–942.
23. Brenner, B., T. Kraft, …, J. M. Chalovich. 1999. Thin filament activation probed by fluorescence of N-((2-(iodoacetoxy)ethyl)-N-methyl) amino-7-nitrobenz-2-oxa-1,3-diazole-labeled troponin I incorporated into skinned fibers of rabbit psoas muscle. *Biophys. J.* 77:2677–2691.
24. Kreutziger, K. L., N. Piroddi, …, M. Regnier. 2011. Calcium binding kinetics of troponin C strongly modulate cooperative activation and tension kinetics in cardiac muscle. *J. Mol. Cell. Cardiol.* 50:165–174.
25. Sun, Y. B., F. Lou, and M. Irving. 2009. Calcium- and myosin-dependent changes in troponin structure during activation of heart muscle. *J. Physiol.* 587:155–163.
26. Fujita, H., D. Sasaki, …, M. Kawai. 2002. Elementary steps of the cross-bridge cycle in bovine myocardium with and without regulatory proteins. *Biophys. J.* 82:915–928.
27. Fujita, H., K. Yasuda, …, S. Ishiwata. 1996. Structural and functional reconstitution of thin filaments in the contractile apparatus of cardiac muscle. *Biophys. J.* 71:2307–2318.
28. Kawai, M., and S. Ishiwata. 2006. Use of thin filament reconstituted muscle fibres to probe the mechanism of force generation. *J. Muscle Res. Cell Motil.* 27:455–468.
29. Lu, X., L. S. Tobacman, and M. Kawai. 2003. Effects of tropomyosin internal deletion Δ23Tm on isometric tension and the cross-bridge kinetics in bovine myocardium. *J. Physiol.* 553:457–471.
30. Bai, F., A. Weis, …, M. Kawai. 2011. Enhanced active cross-bridges during diastole: molecular pathogenesis of tropomyosin's HCM mutations. *Biophys. J.* 100:1014–1023.
31. Spudich, J. A., and S. Watt. 1971. The regulation of rabbit skeletal muscle contraction. I. Biochemical studies of the interaction of the tropomyosin-troponin complex with actin and the proteolytic fragments of myosin. *J. Biol. Chem.* 246:4866–4871.
32. Fujita, H., X. Lu, …, M. Kawai. 2004. The effect of tropomyosin on force and elementary steps of the cross-bridge cycle in reconstituted bovine myocardium. *J. Physiol.* 556:637–649.
33. Chang, A. N., K. Harada, …, J. D. Potter. 2005. Functional consequences of hypertrophic and dilated cardiomyopathy-causing mutations in α-tropomyosin. *J. Biol. Chem.* 280:34343–34349.
34. Opie, L. H., K. R. Mansford, and P. Owen. 1971. Effects of increased heart work on glycolysis and adenine nucleotides in the perfused heart of normal and diabetic rats. *Biochem. J.* 124:475–490.
35. Godt, R. E., and D. W. Maughan. 1988. On the composition of the cytosol of relaxed skeletal muscle of the frog. *Am. J. Physiol.* 254: C591–C604.
36. Kentish, J. C. 1986. The effects of inorganic phosphate and creatine phosphate on force production in skinned muscles from rat ventricle. *J. Physiol.* 370:585–604.
37. Kawai, M., J. S. Wray, and K. Güth. 1990. Effect of ionic strength on crossbridge kinetics as studied by sinusoidal analysis, ATP hydrolysis rate and x-ray diffraction techniques in chemically skinned rabbit psoas fibres. *J. Muscle Res. Cell Motil.* 11:392–402.
38. Kentish, J. C. 1984. The inhibitory effects of monovalent ions on force development in detergent-skinned ventricular muscle from guinea-pig. *J. Physiol.* 352:353–374.
39. Kentish, J. C., H. E. ter Keurs, …, M. I. Noble. 1986. Comparison between the sarcomere length-force relations of intact and skinned trabeculae from rat right ventricle. Influence of calcium concentrations on these relations. *Circ. Res.* 58:755–768.
40. Strang, K. T., N. K. Sweitzer, …, R. L. Moss. 1994. β-Adrenergic receptor stimulation increases unloaded shortening velocity of skinned single ventricular myocytes from rats. *Circ. Res.* 74:542–549.
41. Kawai, M., X. Lu, …, M. W. Wandling. 2009. Tropomyosin period 3 is essential for enhancement of isometric tension in thin filament-reconstituted bovine myocardium. *J. Biophys.* 2009:1–17.
42. Kawai, M., and P. W. Brandt. 1980. Sinusoidal analysis: a high resolution method for correlating biochemical reactions with physiological processes in activated skeletal muscles of rabbit, frog and crayfish. *J. Muscle Res. Cell Motil.* 1:279–303.
43. Kawai, M., Y. Saeki, and Y. Zhao. 1993. Crossbridge scheme and the kinetic constants of elementary steps deduced from chemically skinned papillary and trabecular muscles of the ferret. *Circ. Res.* 73:35–50.
44. Morimoto, S., Q. W. Lu, …, I. Ohtsuki. 2002. Ca^{2+}-desensitizing effect of a deletion mutation ΔK210 in cardiac troponin T that causes familial dilated cardiomyopathy. *Proc. Natl. Acad. Sci. USA.* 99:913–918.
45. Bai, F., H. L. Groth, and M. Kawai. 2012. DCM-related tropomyosin mutants E40K/E54K over-inhibit the actomyosin interaction and lead to a decrease in the number of cycling cross-bridges. *PLoS ONE.* 7:e47471.

46. Zhao, Y., P. M. Swamy, …, M. Kawai. 1996. The effect of partial extraction of troponin C on the elementary steps of the cross-bridge cycle in rabbit psoas muscle fibers. *Biophys. J.* 71:2759–2773.

47. Gordon, A. M., E. Homsher, and M. Regnier. 2000. Regulation of contraction in striated muscle. *Physiol. Rev.* 80:853–924.

48. Geeves, M. A., and S. S. Lehrer. 2002. Cooperativity in the Ca^{2+} regulation of muscle contraction. *Results Probl. Cell Differ.* 36:111–132.

49. Gordon, A. M., M. Regnier, and E. Homsher. 2001. Skeletal and cardiac muscle contractile activation: tropomyosin "rocks and rolls". *News Physiol. Sci.* 16:49–55.

50. McKillop, D. F. A., and M. A. Geeves. 1993. Regulation of the interaction between actin and myosin subfragment 1: evidence for three states of the thin filament. *Biophys. J.* 65:693–701.

51. Pirani, A., M. V. Vinogradova, …, W. Lehman. 2006. An atomic model of the thin filament in the relaxed and Ca^{2+}-activated states. *J. Mol. Biol.* 357:707–717.

52. Sweeney, H. L., H. S. S. Feng, …, H. Watkins. 1998. Functional analyses of troponin T mutations that cause hypertrophic cardiomyopathy: insights into disease pathogenesis and troponin function. *Proc. Natl. Acad. Sci. USA.* 95:14406–14410.

53. Davis, J., S. Yasuda, …, J. M. Metzger. 2012. Diastolic dysfunction and thin filament dysregulation resulting from excitation-contraction uncoupling in a mouse model of restrictive cardiomyopathy. *J. Mol. Cell. Cardiol.* 53:446–457.

54. Gomes, A. V., J. S. Liang, and J. D. Potter. 2005. Mutations in human cardiac troponin I that are associated with restrictive cardiomyopathy affect basal ATPase activity and the calcium sensitivity of force development. *J. Biol. Chem.* 280:30909–30915.

55. Szczesna, D., R. Zhang, …, J. D. Potter. 2000. Altered regulation of cardiac muscle contraction by troponin T mutations that cause familial hypertrophic cardiomyopathy. *J. Biol. Chem.* 275:624–630.

56. Wen, Y. H., Y. Y. Xu, …, W. G. Kerrick. 2009. Functional effects of a restrictive-cardiomyopathy-linked cardiac troponin I mutation (R145W) in transgenic mice. *J. Mol. Biol.* 392:1158–1167.

57. Jacques, A. M., O. Copeland, …, S. B. Marston. 2008. Myosin binding protein C phosphorylation in normal, hypertrophic and failing human heart muscle. *J. Mol. Cell. Cardiol.* 45:209–216.

58. Sadayappan, S., J. Gulick, …, J. Robbins. 2005. Cardiac myosin-binding protein-C phosphorylation and cardiac function. *Circ. Res.* 97:1156–1163.

59. Davis, J., H. Wen, …, J. M. Metzger. 2007. Thin filament disinhibition by restrictive cardiomyopathy mutant R193H troponin I induces Ca^{2+}-independent mechanical tone and acute myocyte remodeling. *Circ. Res.* 100:1494–1502.

60. James, J., Y. Zhang, …, J. Robbins. 2000. Transgenic modeling of a cardiac troponin I mutation linked to familial hypertrophic cardiomyopathy. *Circ. Res.* 87:805–811.

61. Fatkin, D., and R. M. Graham. 2002. Molecular mechanisms of inherited cardiomyopathies. *Physiol. Rev.* 82:945–980.

62. Seidman, J. G., and C. Seidman. 2001. The genetic basis for cardiomyopathy: from mutation identification to mechanistic paradigms. *Cell.* 104:557–567.

63. Knollmann, B. C., S. A. Blatt, …, J. D. Potter. 2001. Inotropic stimulation induces cardiac dysfunction in transgenic mice expressing a troponin T (I79N) mutation linked to familial hypertrophic cardiomyopathy. *J. Biol. Chem.* 276:10039–10048.

64. Kawai, M., R. N. Cox, and P. W. Brandt. 1981. Effect of Ca ion concentration on cross-bridge kinetics in rabbit psoas fibers. Evidence for the presence of two Ca-activated states of thin filament. *Biophys. J.* 35:375–384.

65. Brandt, P. W., R. N. Cox, …, T. Robinson. 1982. Effect of cross-bridge kinetics on apparent Ca^{2+} sensitivity. *J. Gen. Physiol.* 79:997–1016.

66. Solaro, R. J., M. J. Holroyde, J. W. Herzig, and J. Peterson. 1980. Cardiac relaxation and myofibrillar interactions with phosphate and vanadate. *Eur. Heart J.* 1(*Suppl. 1*):21–27.

67. Roth, K., B. Hubesch, …, M. W. Weiner. 1989. Noninvasive quantitation of phosphorus metabolites in human tissue by NMR-spectroscopy. *J. Magn. Reson.* 81:299–311.

68. Layland, J., R. J. Solaro, and A. M. Shah. 2005. Regulation of cardiac contractile function by troponin I phosphorylation. *Cardiovasc. Res.* 66:12–21.

69. Kawai, M., and Y. Zhao. 1993. Cross-bridge scheme and force per cross-bridge state in skinned rabbit psoas muscle fibers. *Biophys. J.* 65:638–651.